

Reduced Magnetization and Loss In Ag-Mg Sheathed Bi2212 wires: Systematics With Sample Twist Pitch and Length

C. S. Myers¹, H. Miao², Y. Huang², M. D. Sumption¹, and E. W. Collings¹

Abstract—Suppression of magnetization and effective filament diameter (d_{eff}) with twisting was investigated for a series of recent Bi2212 strands manufactured by Oxford Superconducting Technologies. We measured magnetization as a function of field (out to 14 T), at 5.1 K, of twisted and non-twisted 37 x 18 double restack design strands. The samples were helical coils 5-6 mm in height and approximately 5 mm in diameter. The strand diameter was 0.8 mm. The magnetization of samples having twist pitches of 25.4, 12.7, and 6.35 mm were examined and compared to non-twisted samples of the same filament configuration. The critical state model was used to extract the 12 T d_{eff} from magnetization data for comparison. Twisting the samples reduced d_{eff} by a factor of 1.5 to 3. The d_{eff} was shown to increase both with L and L_p . Mathematical expressions, based upon the anisotropic continuum model, were fit to the data, and a parameter, γ_2 , which quantifies the electrical connectivity perpendicular to the filament axis, was extracted. The bundle-to-bundle connectivity along the radial axis was found to be approximately 0.2%. The d_{eff} was substantially reduced with L_p . In addition, the importance of understanding sample length dependence for quantitative measurements is discussed.

Index Terms—Bi2212, magnetization, effective filament diameter, high temperature-superconductors, multifilamentary superconductors, superconducting filaments and wires.

I. INTRODUCTION

Bi2212 round wire composite conductors are of great interest for future accelerator applications [1], including for dipole applications as well as muon accelerators. Bi2212 competes with YBCO for these prospective high field applications, where in some cases field quality is important (e.g., dipoles and quadrupoles of future high field accelerators). In magnets where field quality is important, the magnetization of the strand itself is important, and is often discussed in terms of a filament diameter, or an effective filament diameter (d_{eff}), since the magnetization is proportional to d_{eff} [2]. NbTi strands have filament diameters of typically 5 μm or so, and Nb₃Sn, d_{eff} s are typically of order 60 μm . For NbTi, d_{eff} is just the filament diameter, whereas for Nb₃Sn, d_{eff}

is typically the subelement diameter. For Bi2212, it has typically been the case that d_{eff} is the whole filamentary array diameter (the diameter of the strand, excluding the outer sheath), and since the strand ODs are typically 0.8 mm or so, this can lead to d_{eff} s of 500-600 μm . These large values of d_{eff} are caused by small filament-to-filament or bundle-to-bundle outgrowths which occur during the partial melt process heat treatment. These bridges may enhance transport J_c by providing a superconducting path around current limiting mechanisms such as pores and secondary phases [3], but they couple the filaments together and lead to a large d_{eff} [4]-[7].

One method to reduce the hysteresis loss, though not developed specifically to address bridging, is to twist the filaments during manufacture of the wire. Whereas twisting reduces eddy-current loss, it should also reduce the coupling due to bridging because, as the twist becomes tighter (i.e., as the twist pitch length decreases), the number of bridges within the twist pitch length decreases, reducing the amount of transverse current to below the total current which can flow down the length of the sample. Twisting has recently been applied to Bi2212 round wires [8-9], and has indeed been shown to lead to a reduction in AC loss compared to non-twisted samples [8].

Bridging induced magnetization in Nb₃Sn conductors has been seen to depend on sample length (and twist pitch) up to a critical length, at which saturation occurs [10]. Thus, it is not strictly correct to describe the magnetization due to bridging in terms of d_{eff} unless the length dependence is taken into account. Expressions based on the anisotropic critical state (ACS) model which provide quantitative descriptions of bridging in ACS terms, and which account for the length (and twist pitch) dependence, were developed by Sumption [4]. Based on these expressions, bridging induced magnetization is expected to depend linearly on both twist pitch (L_p) and sample length (L) [4]-[7] for shorter L_p and L , with a saturation for large L_p or L .

In this work we measure the magnetization of Bi2212 samples, both twisted and non-twisted. We first confirm the large suppression of magnetization and d_{eff} with the twisting of long non-twisted strands. We then look closer at the functional dependence of d_{eff} on L_p and also L , extracting a parameter, γ_2 , which describes the density of interfilamentary bridges. We can then predict d_{eff} and magnetization based on γ_2 , L_p , and L .

Manuscript received August 11, 2014.

This work was supported by the U.S. Department of Energy, Office of Science, Division of High Energy Physics, under Grant DE-SC0010312 and DE-SC0011721

C. S. Myers, M. A. Susner, M. D. Sumption, and E. W. Collings are with the Center for Superconducting and Magnetic Materials (CSMM), Department of Materials Science and Engineering, The Ohio State University, Columbus, OH 43210 USA (e-mail: myers.1104@osu.edu).

H. Miao and Y. Huang are with Oxford Superconducting Technology, Carteret, NJ, 07008.

II. EXPERIMENTAL

A. Samples

The samples in this work were cut from a multifilamentary Bi2212 strand, which had a Ag-Mg alloy sheath, manufactured by Oxford Superconducting Technologies (OST) [11]-[12]. The strand was 0.813 mm in diameter with 18 bundles, each consisting of 37 filaments (OST 0.8 mm 37 x 18 wire). The bundle diameter was 130 μm , and the filament diameter was 15 μm . The strand was made available in four different segments, each with a different twist pitch, including values of 25.4 mm, 12.7 mm, and 6.35 mm. The fourth segment was not twisted (or infinite L_p). These segments, provided after reaction, were supplied in the form of four helical Bi2212 coils approximately 5 mm in diameter (to fit our PPMS). From these coils, segments were cut for measurement in our PPMS; the maximum coil segment length was 6 mm corresponding to about 5-6 turns. I_c (4.2 K, 12 T) and J_c (4.2 K, 12 T) were measured by OST on a 1 m barrel sample at 12 T, and the values were 130 A and 1050 A/mm², respectively. Embedded in the OST-provided J_c is the OST determined fill factor (via $\lambda_{sc} = I_c/AJ_c$, where A is the cross-sectional area of the strand), such that $\lambda_{sc} = 0.246$. Two different sets of measurements were performed: (i) samples of various L_p (where $L > L_p$), and (ii) non-twisted samples of various lengths (here and throughout L refers to the total strand length, not the length of the coil). The approximate sample length to twist pitch ratio (L/L_p) for the samples with L_p s = 25.4 mm, 12.7 mm, and 6.35 mm was 3, 7, and 12, respectively. Nine different lengths were cut from the non-twisted coil in order to study any length dependence of the magnetization.

B. DC Magnetization Measurements

DC magnetization measurements were performed using DC extraction magnetometry with the ACMS option of a Quantum Design Model 6000 PPMS. 5.1 K $M-B$ loops were measured from -2 to 14 T. The magnetic field was applied to the open face of the coils and was ramped at 13 mT/s.

III. RESULTS AND DISCUSSION

A. 5.1 K $M-B$

The 5.1 K $M-B$ loops of both the twisted and non-twisted samples were obtained by normalizing the measured magnetic moments by the volume of Bi2212 in the samples. The results of the measurements on the twisted samples are shown in Fig. 1 (along with the results of the measurements on the non-twisted samples whose lengths most nearly match the lengths of the twisted samples). The magnetization of the twisted samples is clearly smaller than that of the non-twisted samples (for the same sample length), as we might generally expect, and as demonstrated recently in OST strands [8]. We also notice, however, that the magnetization of the non-twisted samples depends upon sample length. This is further explored in the results of the non-twisted sample measurements shown in Fig. 2. The functional form of both L_p and L dependence are of interest, and we explore this further below.

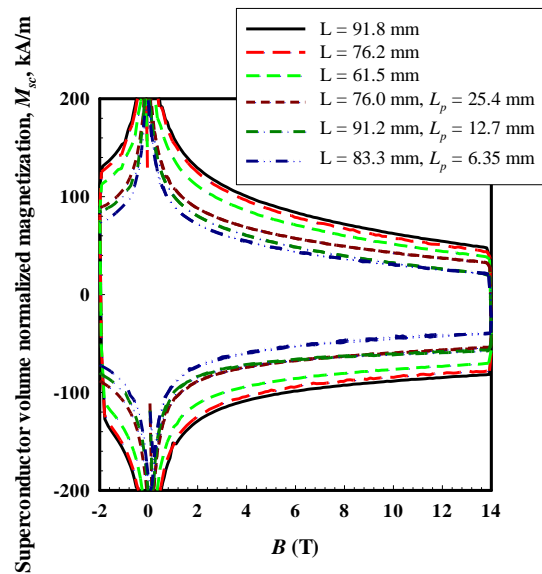


Figure 1. $M-B$ of twisted coil samples with different L_p s plotted alongside $M-B$ s of non-twisted coil samples with similar L . The magnetization of the twisted samples is significantly reduced compared to the non-twisted samples.

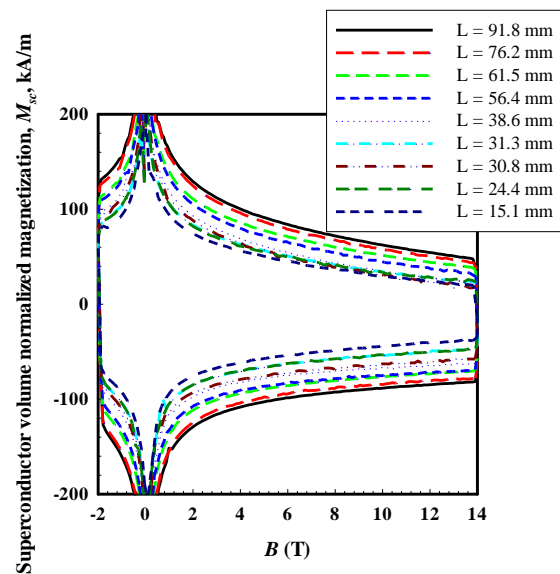


Fig. 2. $M-B$ of non-twisted coil samples with various lengths, L . The magnetization clearly depends upon L .

B. 12 T d_{eff} vs L or L_p

The height of the hysteresis loop (ΔM_{sc}) at 12 T and the transport J_c (4.2 K, 12 T), provided by OST, for a 1 m barrel sample made from the 37 x 18 filament design strand were used as inputs to the standard critical state expression for the J_c of a superconducting rod in a transverse magnetic field

$$d_{eff} = \frac{3\pi\Delta M_s}{4J_c} \quad (1)$$

to calculate d_{eff} at 12 T for all samples. The results are presented in Fig. 3, for all samples, as a function of sample length. The effective filamentary diameters of the twisted samples are substantially smaller than those of the non-twisted

samples at any given sample length. The M - B loops presented in Fig. 1 for the coil samples with L_p s = 6.35 mm, 12.7 mm, and 25.4 mm correspond to the points in Fig. 4 with d_{eff} s of 156, 191, and 211 μ m, respectively.

As noted above, the magnetization also has a length dependence. In fact, the magnetization is linearly dependent upon sample length for the non-twisted set. When comparing twisted and non-twisted samples of similar length, the twisted sample has a greatly reduced d_{eff} and loss compared to the non-twisted sample, consistent with the recent results of Miao *et al* [8]. The linear dependence of sample magnetization on length was predicted by Sumption *et al.* [4]. In that work, a model was developed for Bi2212 magnetization, which predicts an initial linear dependence of magnetization (or d_{eff}) on sample length (of non-twisted samples), with a saturation at long sample lengths, where d_{eff} becomes the filamentary array diameter. A similar dependence of d_{eff} or magnetization on strand twist pitch was predicted, with again a saturation of d_{eff} to the filamentary array diameter. In that work, the strands had relatively high levels of bridging, and saturation occurred at quite small sample lengths, making d_{eff} suppression by strand twisting impractical. The present strands, however, have a slower approach to saturation, making twisting a practical approach for d_{eff} reduction, and implying a lower level of overall bridging. To further illustrate the functional

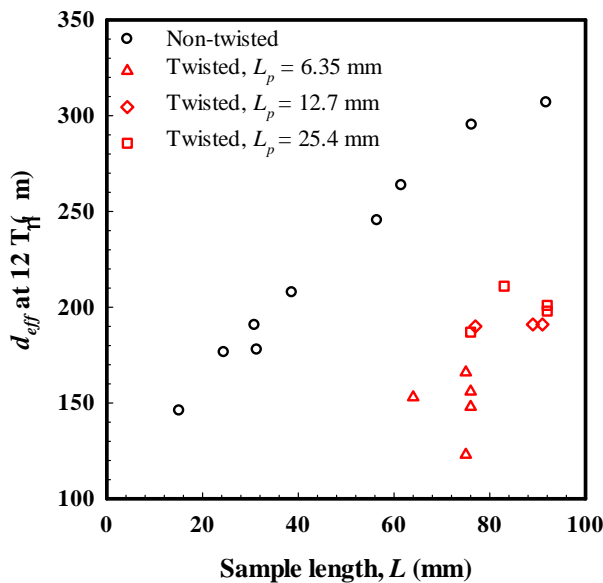


Fig. 3. 12 T d_{eff} vs sample length for twisted and non-twisted samples. d_{eff} of the twisted samples is clearly smaller than that of the corresponding non-twisted sample.

dependence of d_{eff} and magnetization on both L and L_p , the 12 T d_{eff} data for both the non-twisted and twisted coils are re-plotted versus L or L_p , when applicable, in Fig. 4. Here we see an increase in d_{eff} with both L and L_p , as expected from [6]. We can in fact quantify the low level of bridging in the sample by fitting the data of Fig. 4 to the expressions from [6]. We have a much greater number of samples for the non-twisted samples because they could be cut from a single HT sample, whereas samples of different twist pitches require separate

preparation for each pitch value investigated. Given that, we used the non-twisted sample curve for the fit. A linear curve was fitted to the non-twisted coil sample d_{eff} vs L data shown

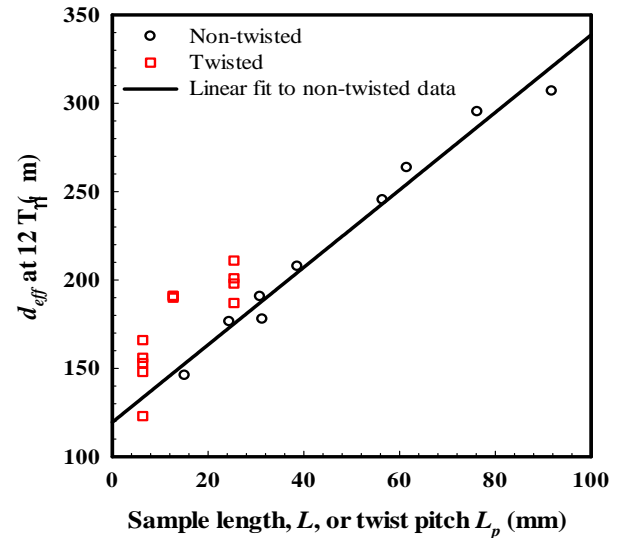


Fig. 4. Dependence of 12 T d_{eff} on sample length or twist pitch length.

in Fig. 4. The slope of this curve is 2.19 μ m/mm and the y-intercept is 119 μ m, which is close to the average bundle diameter of 130 μ m determined using optical microscopy. The value of the y-intercept indicates that the filaments within the bundles are nearly completely coupled (there is dense bridging within the bundles, as expected). In samples of non-zero length, the low level of bridging between the bundles allows some bundle to bundle coupling. As the number of bridges per unit length is fixed, as the sample length increases, there is a linear increase in the total number of bridges which can carry supercurrent through the gap between the bundles, allowing more transverse current flow and therefore increasing the magnetization. The data in Fig. 4 show that the bundles are not completely coupled even for samples up to 92 mm in length, as the d_{eff} at this length is 306 μ m, which is significantly less than the diameter of the entire filamentary array.

As can be seen in Fig. 4 d_{eff} is a function of both L and L_p . From [4] we expect these dependences to be linear. However, the dependence is not exactly the same – a different pre-factor is expected. One reason for this is that the twisted sample has both filamentary J_c and bridging J_c components rotated around the strand by 90° before they are returned across the bridges.

C. Transverse connectivity: extraction of γ_2

The transverse connectivity can be extracted from magnetization measurements. As described in [4] the expression for the incremental magnetization, due to filament bridging, as a function of sample length (or twist pitch length) in the strong coupling (that is, the long sample limit) case is given by

$$\Delta M_s = \frac{4\gamma_1 J_{c1} d_{eff}}{3\pi} \left(1 - \frac{3\pi d_{eff} \beta_c}{32L} \right) \quad (2)$$

where γ_1 is a measure of the connectivity along the length of the sample, $J_{cl,1}$ is the intrinsic critical current density along the length of the sample (normalized to filamentary area), d_{eff} is the effective filamentary diameter, L is the sample length and $\beta_c \equiv J_{cl,1}/J_{c2} = \gamma_1 J_{cl,1}/\gamma_2 J_{cl,2}$, (where J_{cl} is the critical current density along the length of the sample and J_{c2} is the transverse critical current density). For the short sample limit, the modified expression is given by

$$\Delta M_s = \frac{\gamma_2 J_{cl,2} L}{2} \left(1 - \frac{4L}{3\pi\beta_c d_{eff}} \right), \quad (3)$$

where γ_2 is a measure of the connectivity across the sample and $J_{cl,2}$ is the intrinsic critical current density across the sample (normalized to filamentary area).

At the critical length, L_{crit} , which is the length at which the magnetization just saturates, the two above equations can be set equal. In fact, if we wish to only extract the initial slope of (3), we can simply equate the first terms of each, obtaining

$$\frac{4\gamma_1 J_{cl,1} d_{eff}}{3\pi} = \frac{\gamma_2 J_{cl,2} L_{crit}}{2} \quad (4)$$

To use this equation as is, it is necessary to make some assumptions. If we make the assumptions that the current density is isotropic (i.e., $J_{cl,1} = J_{cl,2}$) and the sample has a uniform J_c along its length (i.e., it is fully connected along its length and $\gamma_1 = 1$), we can extract the transverse electrical connectivity, γ_2 . We get

$$\gamma_2 = \frac{4}{\pi} \frac{2}{3} \frac{d_{eff}}{L_{crit}}. \quad (5)$$

In fact, if we assume that the d_{eff} vs L plot is linear until it reaches saturation, this expression is simply the slope of the linear (and below saturation) region of the plot. If we substitute the slope of 2.19×10^{-3} , for d_{eff}/L , we get $\gamma_2 = 1.86 \times 10^{-3}$. That is, about 0.2% of the area between the bundles should be spanned by bridges.

If we rearrange (1) to get an expression for ΔM_s and then substitute this expression into (2), we can use the first (linear) part of (2) to get an estimate for the transverse electrical connectivity. However, we note that (2)-(3) are expressions for the incremental magnetization with L , and do not represent the total magnetization of the sample. That is, they do not take into account the offset magnetization coming from the magnetization of the filaments themselves. In fact, Fig. 4 shows that there is an offset (y-intercept) of 119 μm , which is significantly larger (~ 8 times) than the green state filamentary diameters, and indicates that the filaments start out coupled to approximately this length scale (i.e., the subelements are coupled within themselves). To obtain an expression for the total magnetization, including the magnetization of the (coupled) filaments themselves, (2)-(3) should be modified by adding on the offset term. If we do this when we substitute (1)

into (2) as outlined above, the expression becomes

$$\frac{4d_{eff}J_c}{3\pi} = \frac{\gamma_2 J_{cl,2} L}{2} + \frac{4d_{bundle}J_c}{3\pi}. \quad (6)$$

where d_{bundle} ($= 119 \mu\text{m}$, in this case) is the diameter of subelement bundles (i.e., $d_{subelement}$). To extract γ_2 from this expression, we must assume that the critical current density down the length of the filament equals the intrinsic transverse critical current density (i.e., $J_c = J_{cl,2}$). Now, rearranging and solving for γ_2 gives

$$\gamma_2 = \frac{8(d_{eff} - d_{bundle})}{3\pi L}. \quad (7)$$

Table I gives the results of using this expression to calculate γ_2 for all of the non-twisted sample lengths.

Table I. γ_2 extracted using linear part of equation 3.

Length (mm)	d_{eff} (μm)	γ_2 ($\times 10^{-3}$)
92	307	1.74
76	295	1.96
62	264	2.00
56	245	1.89
39	208	1.95
31	178	1.60
31	191	1.98
24	176	1.98
15	146	1.52

In Table 1, we show the extracted γ_2 for non-twisted samples of different length. If the assumptions we used to extract γ_2 are correct, it represents the fraction of the longitudinal cross-sectional area of the strand which contains bridges. This should be an intrinsic property of the strand and should not depend on the sample length.

IV. CONCLUSION

In this work we measured the suppression of magnetization and d_{eff} with twisting for an OST manufactured 0.8 mm 37 x 18 Bi2212 strand. Magnetization and d_{eff} values were suppressed by factors of 1.5-3, making d_{eff} and magnetization 1.5-3 times smaller for twisted samples as compared to non-twisted samples. This effect was further systemized and quantified by looking at the dependence of d_{eff} on L_p , and also the dependence of d_{eff} on L . A model was applied which described the linear dependence on both L and L_p , and extracted a value for the connectivity parameter γ_2 ; a value of only 0.2% was found between the subelements. We conclude that (1) loss, magnetization, and d_{eff} are suppressed by sample twisting, (2) it is possible to quantify this effect by a parameter γ_2 , and (3) it is important to have long samples ($L \gg L_p$, and also $L > L_{crit}$) to obtain results most relevant to application.

ACKNOWLEDGMENT

The authors thank Dr. Milan Majoros for helpful discussion.

REFERENCES

- [1] A. Godeke *et al.*, "Progress in Wind-and-React Bi2212 Accelerator Magnet Technology," *IEEE Trans. Appl. Supercond.* vol. 19, pp. 2228-2231, 2009.
- [2] A. K. Ghosh, K. E. Robins, and W. B. Sampson, Arnold, "Magnetization measurements on multifilamentary Nb₃Sn and NbTi conductors," *IEEE Trans. Magn.* vol. 21, pp. 328-331, 1985.
- [3] T. Shen *et al.*, "Filament to filament bridging and its influence on developing high critical current density in multifilamentary Bi₂Sr₂Ca₁Cu₂O_x round wires," *Supercond. Sci. Technol.*, vol. 23, 025009, 2009.
- [4] M. D. Sumption, "A model for bridging and coupling in superconductors," *Physica C*, vol. 261, pp. 245-258, 1996
- [5] M. D. Sumption, L. R. Motowidlo, and E. W. Collings "Determination of the true (or potential) transport-Jc of a multifilamentary Bi:HTSC/Ag strand in the presence of bridging and generalized sausaging," *Physica C*, vol. 291, pp. 267-271, 1997.
- [6] C. S. Myers *et al.*, "Transport, magnetic, and SEM characterization of a novel design Bi-2212 strand," *IEEE Trans. Appl. Supercond.* vol. 21, pp. 2804-2807, 2011.
- [7] S. Kasai *et al.*, "Magnetization property of Bi-2212 round wires," *IEEE Trans. Appl. Supercond.* vol. 14, pp. 1098-1101, 2004.
- [8] H. Miao, Y. Huang, S. Hong, M. Gerace, and J. Parrell, "Bi2212 round wire development for high field applications," in 11th European Conference on Applied Superconductivity (EUCAS2013) *Journal of Physics Conference Series* vol. 57, 022020, 2013.
- [9] Y. Huang, H. Miao, S. Hong, and J. A. Parrell, "Bi-2212 round wire development for high field applications," *IEEE Trans. Appl. Supercond.* vol. 24, 06400205, 2014.
- [10] R. B. Goldfarb and K. Itoh, "Reduction of interfilament contact loss in Nb₃Sn superconductor wires," *Journal of Appl. Physics* vol. 75, pp. 2115-2118, 1994.
- [11] H. Miao, *et al.*, "Development of round multifilament Bi-2212/Ag wires for high field magnet applications," *IEEE Trans. Appl. Supercond.* vol. 15, 2554-2557, 2005.
- [12] H. Miao, Y. Huang, M. Meinesz, S. Hong, and J. A. Parrell, "Development of Bi-2212 round wires for high field magnet applications," *Adv. In Cryo. Eng.* Vol. 58 pp. 315-323 2012.